SIMULATION OF THE PLASMA BEATWAVE ACCELERATOR

D. J. Sullivan and B. B. Godfrey
Mission Research Corporation, Albuquerque, New Mexico 87106

ABSTRACT

One-dimensional relativistic and electromagnetic simulations show the Plasma Beatwave Accelerator to be a viable approach to obtaining large accelerating fields. The plasma wave excited by Raman Forward Scattering has a longitudinal electric field on the order of 100 MeV/cm to 10 GeV/cm based on plasma densities of 10^{16} cm^{-3} to 10^{20} cm^{-3}. The use of optical mixing to grow a plasma wave of the proper frequency above the noise level greatly reduces the laser intensity needed to drive the Raman instability. TeV energies for plasma electrons or pre-accelerated charged particles in short distances appear feasible. Wave synchronism is maintained in space and time provided the laser beatwave intensity is properly chosen. Streaming instabilities may be overcome in the same manner. The frequency matching condition appears less strenuous than anticipated. Two- and three-dimensional effects must still be resolved.

INTRODUCTION

The Plasma Beatwave Accelerator[1,2] is one of a number of particle accelerator concepts utilizing the high fields inherent in intense laser beams. In this case, EM waves interact nonlinearly with an underdense plasma through optical mixing or Raman Forward Scattering (RFS) to excite large amplitude plasma waves. The plasma self-fields provide the acceleration. Thus, the concept is a collective effect accelerator. The longitudinal electrostatic field of the plasma depends on the plasma density and is typically on the order of $mc\omega_p/e$, where m is the electron rest mass, e is the electron charge, c is the speed of light and ω_p is the electron plasma frequency. For a 10^{18} cm^{-3} plasma this expression is equal to 1 GeV/cm. It explains the very high accelerating fields obtainable with this mechanism.

The Plasma Beatwave Accelerator can be used in two different regimes. In one case preaccelerated and bunched particles are injected into the plasma. If streaming instabilities can be suppressed, a low emittance TeV beam can be generated in a relatively short distance. This scheme, however, requires many plasma stages in order to obtain this high energy. A second regime relies on a single plasma region. A high intensity laser pulse would result in a large flux of particles with an exponential energy distribution up to several GeV. The maximum energy in the distribution is adjustable by varying the ratio of ω/ω_p as noted below. This paper will concentrate on the former application.

Because previous papers,[3-5] cover the theory in detail, we will only briefly describe the acceleration mechanisms before discussing the simulations. Our results address optical mixing, Raman Forward Scattering, wave synchronism and frequency matching. A simulation which coinjects an electron beam with the laser pulse will be described in detail.

ACCELERATION MECHANISM

The process depends upon the interaction between an intense electromagnetic wave and the electrons of an underdense plasma. The nonlinear ponderomotive force associated with the light wave's propagation in the plasma displaces the electrons. Note that the ponderomotive force of interest is in the direction of propagation as shown in Fig. 1 and not transverse to the pulse. This leads to a charge separation and coincident restoring force producing a train of plasma oscillations. The phase velocity of the wake plasma wave is equal to the group velocity of the EM wave, which is derived from the dispersion relation $\omega^2 = k^2c^2 + \omega_p^2$ to be

$$\omega_p/k_p = v_p = v_g = (1 - \omega_p^2/\omega^2)^{1/2}\, c, \qquad (1)$$

where k_p is the plasma wavenumber, v_p the plasma wave phase velocity, v_g the EM wave group velocity, and ω and ω_p the EM and plasma wave frequencies, respectively. Because of the mobility of electrons, and the fact that large changes in energy for relativistic electrons translate into small velocity changes, the electrons are synchronous with the wave front for long periods.

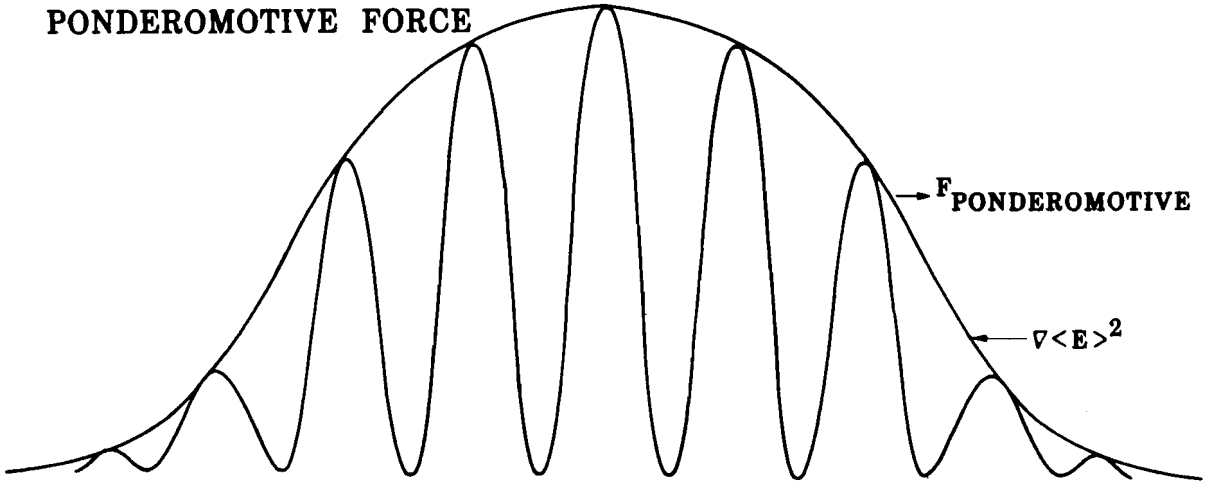

Figure 1. Schematic of a laser pulse indicating the axial ponderomotive force due to the intensity gradient.

In the wave frame the electrostatic field associated with the plasma can be viewed as a particle mirror with the maximum acceleration taking place when the electron experiences a momentum change of $2\gamma\beta mc$, where β is the wave velocity normalized to c and γ is the usual relativistic factor given by $(1 - \beta^2)^{-1/2}$. Transforming back to the laboratory frame yields a maximum electron energy of $\gamma^{max}mc^2$ where $\gamma^{max} = 2\omega^2/\omega_p^2$. The plasmon electric field derived from trapping arguments is $E_z = mc\omega_p/e$, which implies an accelerating field on the order of a GeV/cm for a 10^{18} cm^{-3} plasma density. Table 1 presents scalings for various quantities of interest based on the plasma density and laser frequency. Relativistic effects are not taken into account.[5,6] One can determine a relationship for the minimum laser E-field amplitude, E_0^{min}, needed to capture electrons at rest in the lab frame from trapping arguments and the nonlinear ponderomotive force equations.[5,6] However, since this relationship is not a prerequisite for preaccelerated injected particles, its derivation will not be reviewed here.

TABLE 1

Parameter	Value	Scaling with density
Maximum Energy	$2(\omega/\omega_p)^2$	n^{-1}
Saturated Electrostatic Field	$mc\omega_p/e$	$n^{1/2}$
Acceleration Length	$2(\omega/\omega_p)^2\ c/\omega_p$	$n^{-3/2}$
Acceleration Time	$2(\omega/\omega_p)^2\ 1/\omega_p$	$n^{-3/2}$

MICROWAVES

Since the concept presented here is valid for any frequency EM radiation, microwaves were considered as a possible source. There are several advantages. Because the frequency is lower, the minimum intensity requirement to trap electrons from rest is decreased. The lower frequency also decreases the plasma density necessary to produce the same ω/ω_p ratio. Finally, the use of a waveguide would ensure a constant minimum focal area for a length sufficient to saturate the acceleration process. This is the same as stating that the diffraction problem associated with focusing a laser to a small spot size ($r \sim \lambda$) in a plasma would be overcome. Unfortunately, even the lower power requirement

(tens of Gigawatts) is beyond the capability of present microwave devices. Furthermore, rather than being advantageous the use of a waveguide is a severe drawback.

The dispersion relation for an EM wave in a plasma filled waveguide is $\omega^2 = k^2c^2 + \omega_p^2 + \delta^2c^2/R^2$. Thus the group velocity is

$$v_g = \left(1 - \frac{\delta^2c^2}{\omega^2R^2} - \frac{\omega_p^2}{\omega^2}\right)^{1/2} c \qquad (2)$$

where R is the guide tube radius and δ is the appropriate Bessel Function zero for the waveguide mode being generated. It is readily seen that the group velocity of a microwave in the waveguide will be substantially less than in a homogeneous medium. Also recall that $\gamma^{max} = 2\gamma^2$, but γ no longer equals ω/ω_p. Instead it is given by

$$\gamma = \frac{\omega}{(\delta^2c^2/R^2 + \omega_p^2)^{1/2}} \qquad (3)$$

Taking currently available magnetron experimental parameters used for the generation of a TE_{01} wave ($\omega = 2\times10^{10}$, $\delta = 3.83$, $R = 10.2$ cm) and assuming $\omega \gg \omega_p$ and a power level large enough to induce particle trapping, the maximum electron energy is given by $\gamma^{max} = 2\gamma^2 = \omega^2R^2/\delta^2c^2 = 6.3$. This result is verified in a fully two-dimensional particle simulation in cylindrical geometry where $\omega = 3.0\ \omega_p$, $R = 10.2$ cm, $\delta = 3.83$ and $E_0 = 4\sqrt{2}\ mc\omega/e$ using an instantaneous risetime and $\tau_{pulse} = \pi/\omega_p$. The resulting TE_{01} wave generated maximum electron energies of $\gamma^{max} = 7.8$. The actual γ^{max} from equation 3 is 4.7.

We do not wish, however, to rule out the possibility of performing useful microwave experiments on this concept. By using the process of optical mixing, described below, preaccelerated charged particles or a hot plasma, and higher order waveguide modes, interesting laboratory experiments might be performed. Of interest is the suggestion made at this conference to conduct microwave experiments in the ionosphere. A uniform plasma density available in various ionosphere layers would be extremely useful.

SIMULATIONS

Simulations were carried out using a two-dimensional, fully relativistic and electromagnetic particle-in-cell code. The code can solve self-consistently for the time dependent trajectories of tens of thousand of plasma particles over thousands of plasma periods. All variables are expressed in dimensionless terms. Therefore, length is in units of c/ω_p; time is measured in units of ω_p^{-1}; and particle velocity is given by $v_i = \beta_i\gamma$ ($i = 1, 2, 3$), where ω_p is the initial electron plasma frequency.

In simulations on the Beatwave Accelerator two plane-polarized electromagnetic waves are launched into a Cartesian geometry. Periodic boundary conditions in the transverse (y) direction make configuration space effectively one-dimensional. In general, the simulation has 1250 cells in the longitudinal (z) direction modelling a length of 100 c/ω_p. The cells in the y direction appeared uniform because of periodicity. Each of these macrocells initially contained 24 particles. The risetime of the laser pulses was typically 25 ω_p^{-1}. The were ions taken to be an infinitely massive neutralizing background except in one run. Different simulations were made in which the values of ω_0/ω_p, ω_1/ω_p, E_0 and electron temperature, T_e, were varied where ω_0 and ω_1 are the two laser frequencies.

Usually, a vacuum region of 10π c/ω_p long was left between the left hand boundary and the plasma in order to accurately determine the dynamics of laser injection into the plasma. When the laser pulse encounters the plasma, the nonlinear ponderomotive force resulting from the intensity gradient causes the electrons to snowplow. This continues until the force arising from charge separation is greater than the ponderomotive force, and the electrons attempt to restore the charge imbalance by moving in the negative z direction. This motion initiates a train of large amplitude plasma waves.

The one drawback evident in the single wavepacket scheme[1,5] was the short pulse ($\tau < 2\pi\ \omega_p^{-1}$). This implied an instantaneous risetime to very high intensities. It is obviously unattainable. The beatwave approach, on the other hand, is a practical means of obtaining the required intensity gradient necessary for the nonlinear ponderomotive force to establish large amplitude plasma waves. The beatwave results from two parallel coherent EM sources ω_0 and ω_1 where $\omega_0 - \omega_1 = \omega_p$. This can be accomplished by utilizing two separate colinear lasers or exciting two appropriate bands of the same laser.[3] An example

of the resultant wave pattern is given in Figure 2 where $\omega_0 = 10.6$ ω_p and $\omega_1 = 9.6$ ω_p. Figure 2 is a probe history of the combined laser electric fields and their power spectrum at injection. Each wave trough has a length $\lambda_p/2 = \pi\ c/\omega_p$ in which to trap particles and accelerate them up to a maximum energy of[2]

$$\gamma^{max} = 2\gamma^2 = 2[1 - (\omega_0 - \omega_1)^2/(k_0 - k_1)^2c^2]^{-1} \qquad (4)$$

where k_0 and k_1 are the respective EM wavenumbers in the plasma. Equation (2) is approximately the old expression $\gamma^{max} = 2(\omega_0/\omega_p)^2$ for $\omega_0, \omega_1 \gg \omega_p$.

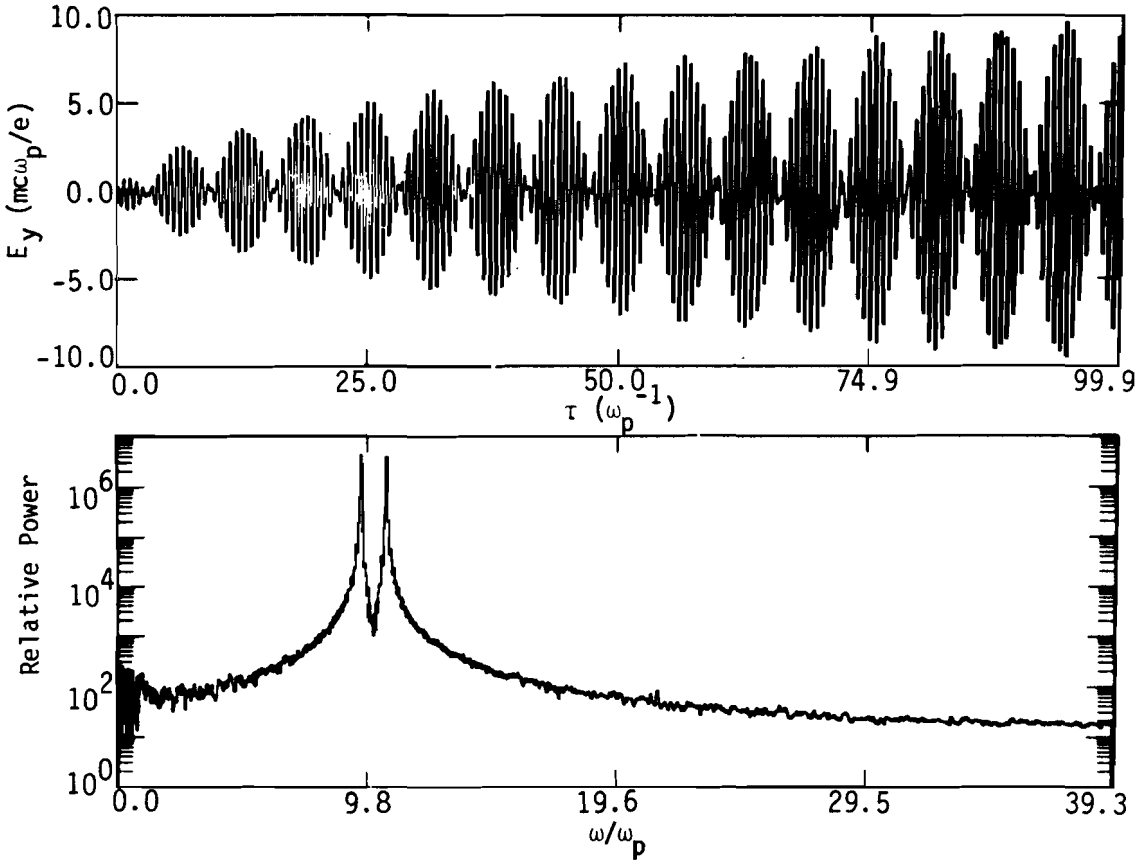

Figure 2. Time history and power spectrum at injection of the two plane polarized laser electric fields. Simulation parameters are $\omega_0 = 10.6\ \omega_p$, $\omega_1 = 9.6\ \omega_p$ and $E_0\ (0,1) = 5.0\ mc\omega_p/e$.

NONLINEAR WAVE-WAVE PROCESSES

An alternative method of depicting the beatwave acceleration is in terms of two nonlinear wave-wave interactions. At low intensities where $E_o\ (0,1) \ll mc\omega\ (0,1)/e$ optical mixing can result in large amplitude plasma waves.[7,8] This occurs provided $\omega_p = \omega_o \pm \omega_1$. Then, the beat frequency of the electromagnetic waves is in resonance with the plasma, and electron density fluctuations can grow. The result is linear growth of the plasma wave amplitude in time until relativistic plasma effects cause a frequency mismatch and wave saturation.

The second interaction is the Forward Raman Scattering Instability.[1,2,9] As the laser waves transit the plasma, they undergo successive scatterings where $\omega_n = \omega_o - n\omega_p$. Alternatively, this may be viewed as $k_n = k_o - nk_p$. This is a parametric three-wave process where a large electromagnetic wave interacts with a plasma to generate another forward moving electromagnetic wave and a plasma wave. Conservation of energy and momentum require the frequency and wavenumber matching conditions noted above. As is usual for parametric processes, the pump wave must exceed a certain intensity threshold for the instability to take place.[10]

The two wave-wave interactions, however, are not mutually exclusive - one limited to low intensities and the other to high. Rather, the plasma wave excited by optical mixing helps drive the parametric instability. To examine this a simulation with $v_{osc}\ (0,1)/c \equiv eE_o(0,1)/mc\omega(0,1) = .04$ and $.05$ was conducted. The plasma was cold at $\omega_p\tau = 0$. The linear growth of the plasma wave is depicted in Figure 3. At this time ($\omega_p\tau = 150$) the density fluctuations are 10% of the initial density. The analytical equation[8] indicates saturation should occur at a fluctuation level of 5%. Indeed, time histories of the laser fields indicate a cascade to lower frequencies in steps of ω_p indicative of an RFS instability. By $\omega_p\tau = 300$ the plasma field amplitude has saturated at $.2\ mc\omega_p/e$, the density variations are as high as .75 of the initial value, and the RFS instability is fully developed as seen in Figure 4. However, as expected, these field levels are not sufficient to trap plasma electrons at rest.

The importance of this result must be stressed. It indicates that large amplitude plasma waves can be grown from relatively low intensity laser sources, due to RFS excitation by optical mixing. Consider the cold plasma simulation just discussed. If ω_o is 2.36×10^{14} sec^{-1} (λ_o

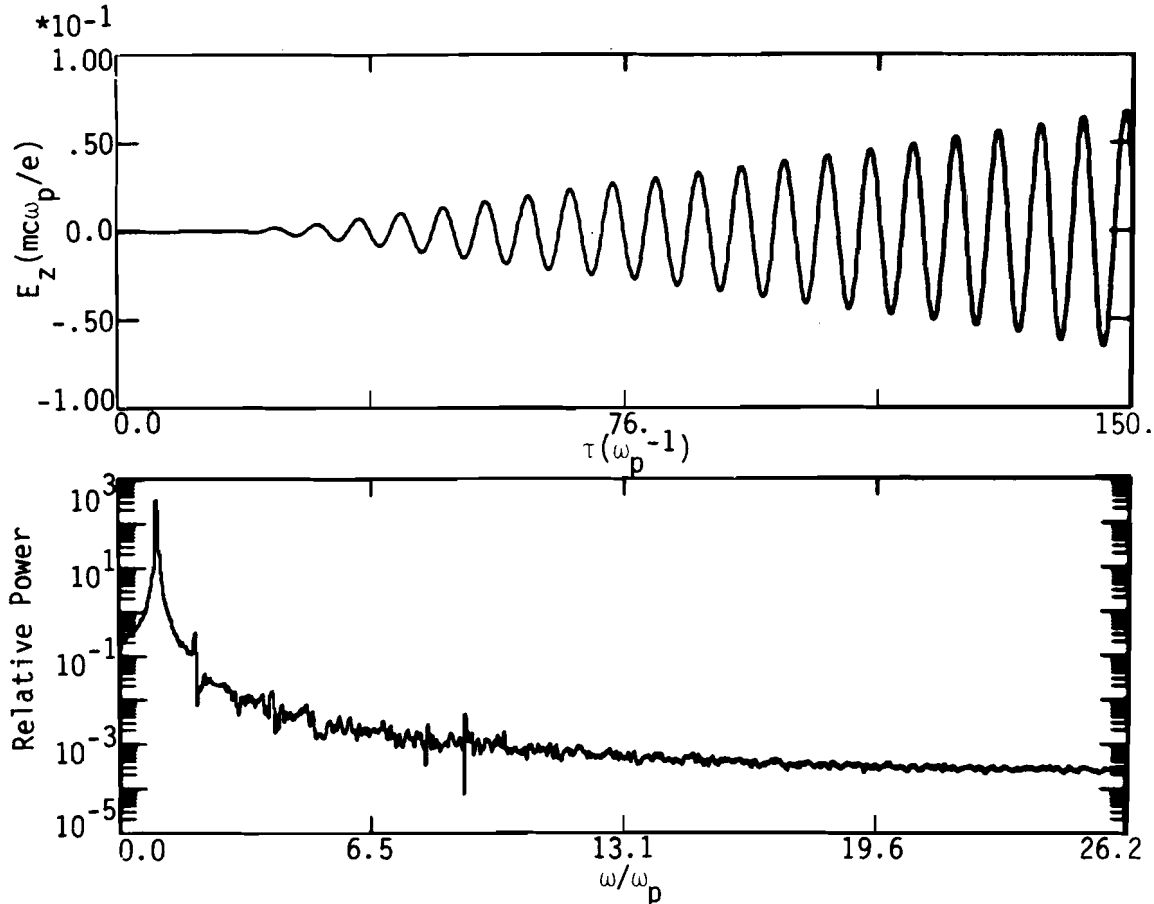

Figure 3. Time history and power spectrum inside the plasma of the longitudinal electric field. Simulation parameters are $\omega_o = 5.0\ \omega_p$, $\omega_1 = 4.0\ \omega_p$ and $E_o\ (0,1) = 0.2\ mc\omega_p/e$.

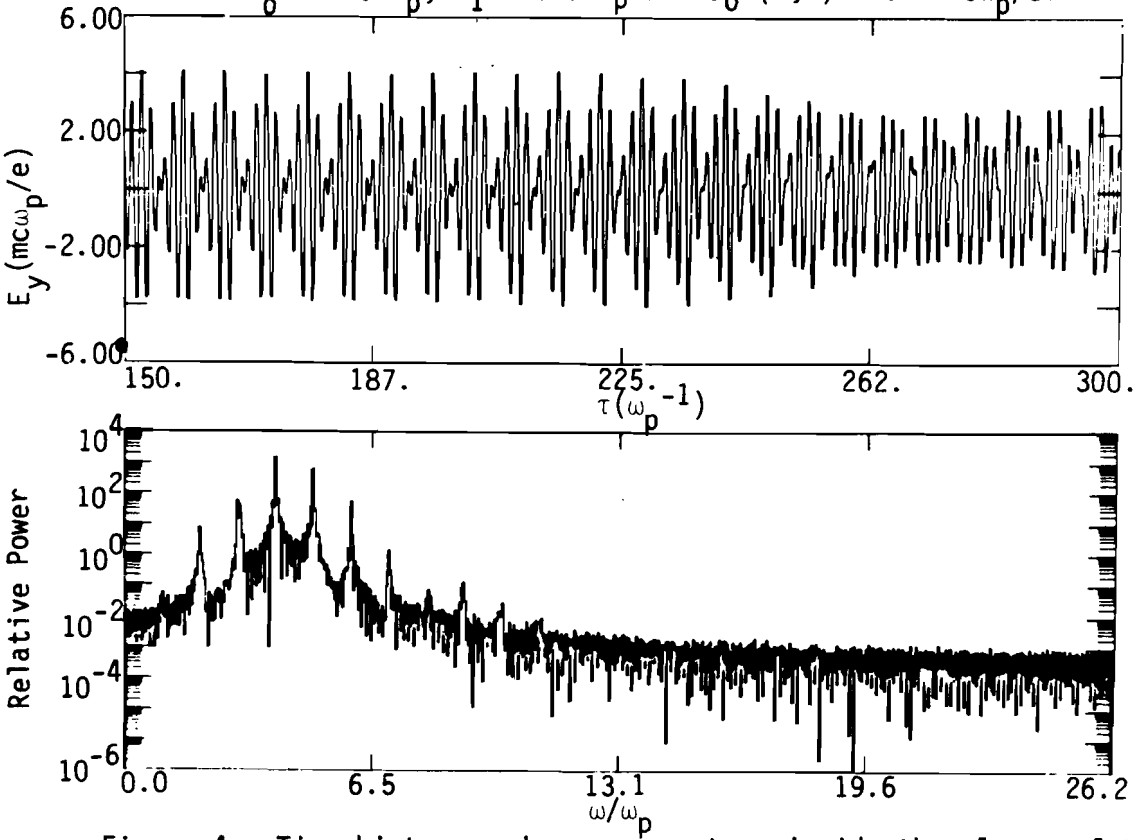

Figure 4. Time history and power spectrum inside the plasma of the combined laser electric field. Simulation parameters are $\omega_o = 5.0\ \omega_p$, $\omega_1 = 4.0\ \omega_p$ and $E_o\ (0,1) = 0.2\ mc\omega_p/e$.

= 10 μm), then λ_1 is 8 μm and the plasma density is 7×10^{17} cm^{-3}. The equivalent laser intensity is only 1.3×10^{14} W/cm^2, yet the plasma wave accelerating field is 166 MeV/cm.

This lower intensity makes the Plasma Beatwave Accelerator an extremely attractive candidate for application to high energy physics accelerators. The lower intensity implies the focal spot size may be larger, thus lessening diffraction of the laser pulse in the plasma. The fact that plasma electrons are not trapped is advantageous for injection of preaccelerated, bunched particles. As will be seen in the next section, large numbers of trapped particles lead to wave damping and loss of synchronism.

In a subsequent simulation where E_0 (0,1) were each reduced by a factor of 2 and T_e = 10 keV, neither optical mixing nor RFS was evident. This was apparently due to high frequency density spikes in the hot plasma. Theory predicts that plasma inhomogeneity raises the RFS threshold and inhibits optical mixing.

At higher intensities the RFS instability grows exponentially to a saturation level. Figure 5 depicts the plasma wave amplitude and spectrum for the case of v_{osc} (0,1)/c ~ 0.5. Note the presence of spectral components at $\omega = \omega_0 + \omega_1$ as well as $\omega = \omega_0 - \omega_1 = \omega_p$ and higher harmonics. Graphic evidence of this instability is also given in Figure 6, which is the time history and power spectra of the laser waves inside the plasma. This downward cascade of energy into multiples of ω_p is a clear signature of Raman instability. The upward cascade is the result of multiple four-wave interactions in which each wave is coupled to all other waves in a multiwave parametric process.[11] The sidebands are often referred to as Stokes (downshifted) and Anti-Stokes (upshifted) lines.

This simulation is particularly interesting, because the parameters model a CO_2 laser emitting in the 9.6 μm and 10.6 μm bands at a combined intensity of 1.3×10^{16} W/cm^2. The laser pulse is incident on a hot 10^{17} cm^{-3} plasma. Excitation of these CO_2 lines at this intensity and production of such a plasma is not beyond current technology. The higher saturation level of the electrostatic field is only a factor of three larger in this simulation than in the run where optical mixing was important. This implies a field of 316 MeV/cm based on the lower plasma density. The combined laser intensities here, however, are equivalently 100 times larger. Nevertheless, there are some advantages to this higher intensity.

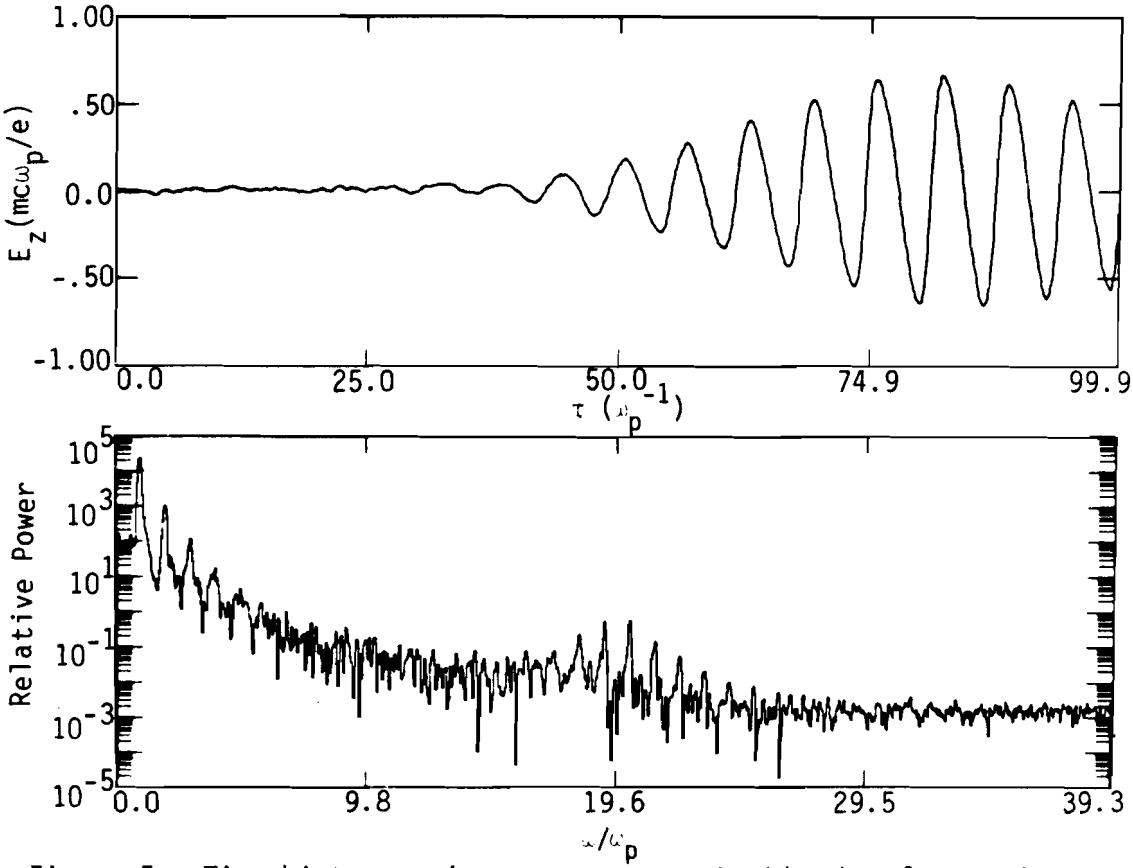

Figure 5. Time history and power spectrum inside the plasma of the longitudinal electric field. Simulation parameters are ω_o = 10.6 ω_p, ω_1 = 9.6 ω_p and E_o (0,1) = 5.0 $mc\omega_p/e$.

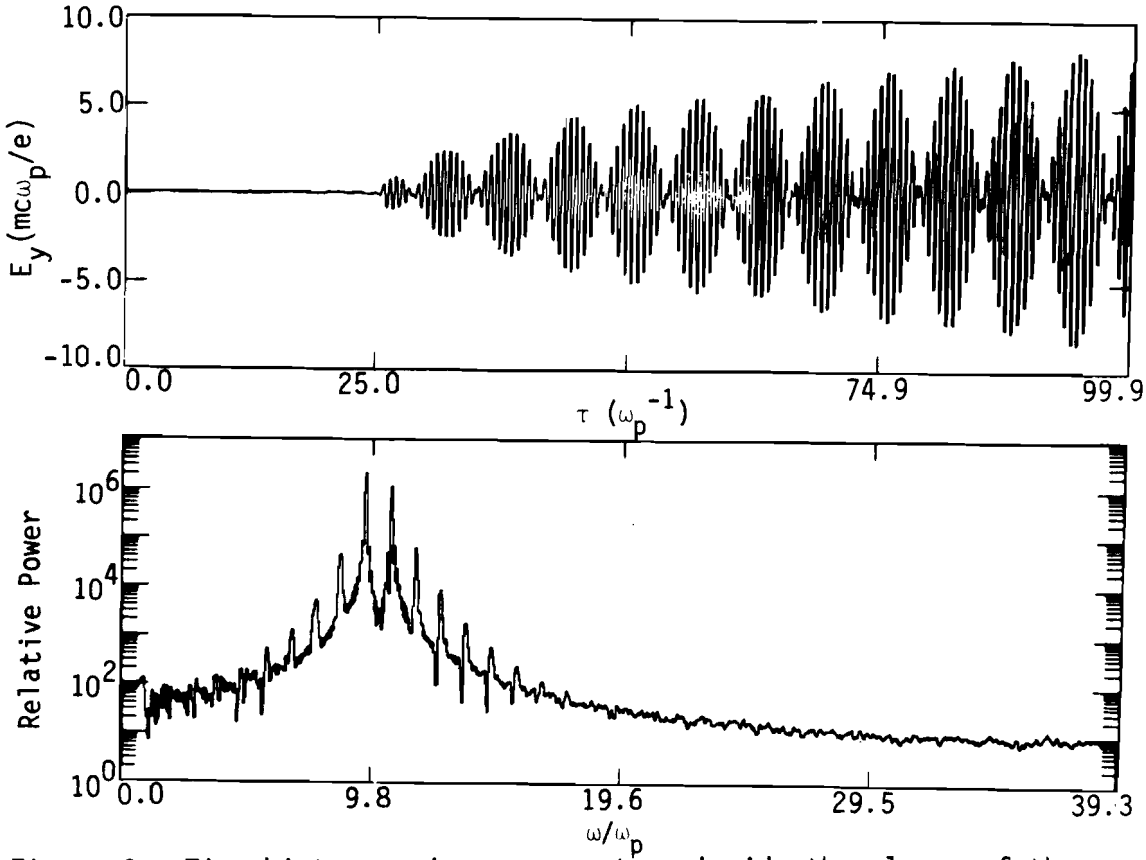

Figure 6. Time history and power spectrum inside the plasma of the two plane polarized laser wave electric fields. Parameters are ω_o = 10.6 ω_p, ω_1 = 9.6 ω_p and E_o (0,1) = 5.0 $mc\omega_p/e$.

The high value of v_{osc}/c and its associated relativistic effects lead to particle trapping and acceleration of a small number of electrons. This also occurs if $T_e = 0$ for the same parameters. The trapped particles originate at wavelength intervals where $\beta_y\gamma$ is a maximum and are not associated with any overall temperature. These results are important if the plasma is to be the source of accelerated particles. In addition, the particle bunching at higher intensity is more pronounced and coherent. As a reference, assume the focal spot size for the laser pulse described above is 10^{-4} cm^2. Then, based on simulation results, a particle pulse occurs every .18 psec, contains 5×10^{10} electrons, carries a peak current of 96 kA at a current density of 960 Megamps/cm^2 (see Figure 7). The main reason for belaboring this point is to indicate the potential the plasma has for confining and accelerating high density bunches of preaccelerated ions. Finally, consider the plasma electron distribution function reproduced in Figure 8. The monotonically decreasing distribution functions are absolutely stable against streaming instabilities. This will be covered in more detail later.

WAVE SYNCHRONISM

In order for plasma electrons or preaccelerated particles to attain the maximum acceleration given by $\gamma^{max} \sim 2(\omega/\omega_p)^2$, they must maintain synchronism with the wave for a distance on the order of $\gamma^{max}c/\omega_p$. A number of processes may be involved in destroying wave coherence. All result from driving plasmas with very intense laser pulses. The effects are seen in a simulation where the combined $v_{osc}/c > 1$.

By far the main degradation results from too many trapped particles. As the amplitude of the plasma wave increases, more particles can be trapped and nonlinear damping of the wave results as energy is transferred to the particles.[13] A slight increase in the trapping width of the wave,[3,4] exponentially increases the number of trapped particles in a thermal distribution. Simulation movies confirm that they are executing trapping oscillations which damp the plasma waves. This leads to incoherent density fluctuations and turbulent heating which makes the plasma nonuniform. If this changes the plasma dispersion relation appreciably, the frequency matching condition will be upset.

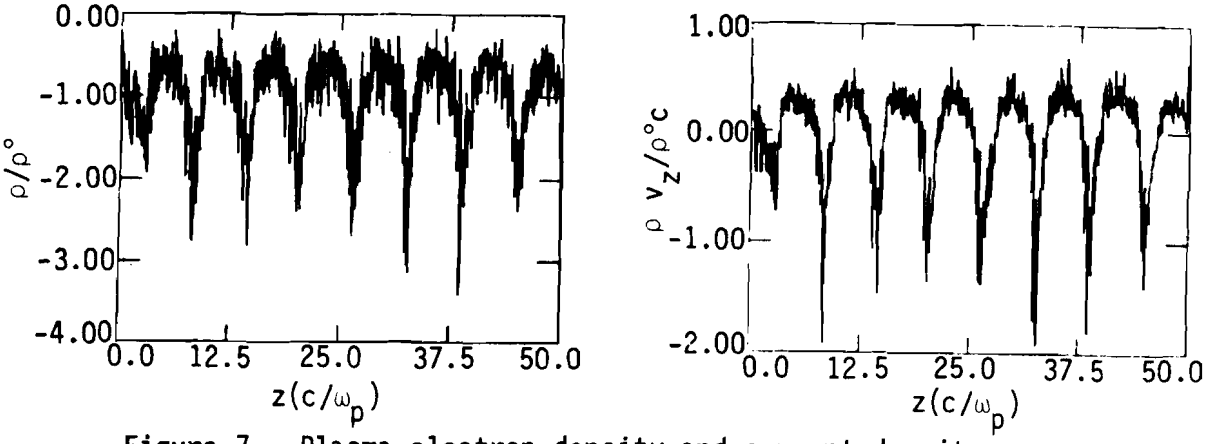

Figure 7. Plasma electron density and current density normalized to initial electron density versus longitudinal distance at $\tau = 70\ \omega_p^{-1}$. Simulation parameters are $\omega_0 = 10.6\ \omega_p$, $\omega_1 = 9.6\ \omega_p$, $E_0\ (0,1) = 5.0\ mc\omega_p/e$ and $T_e = 0$ keV.

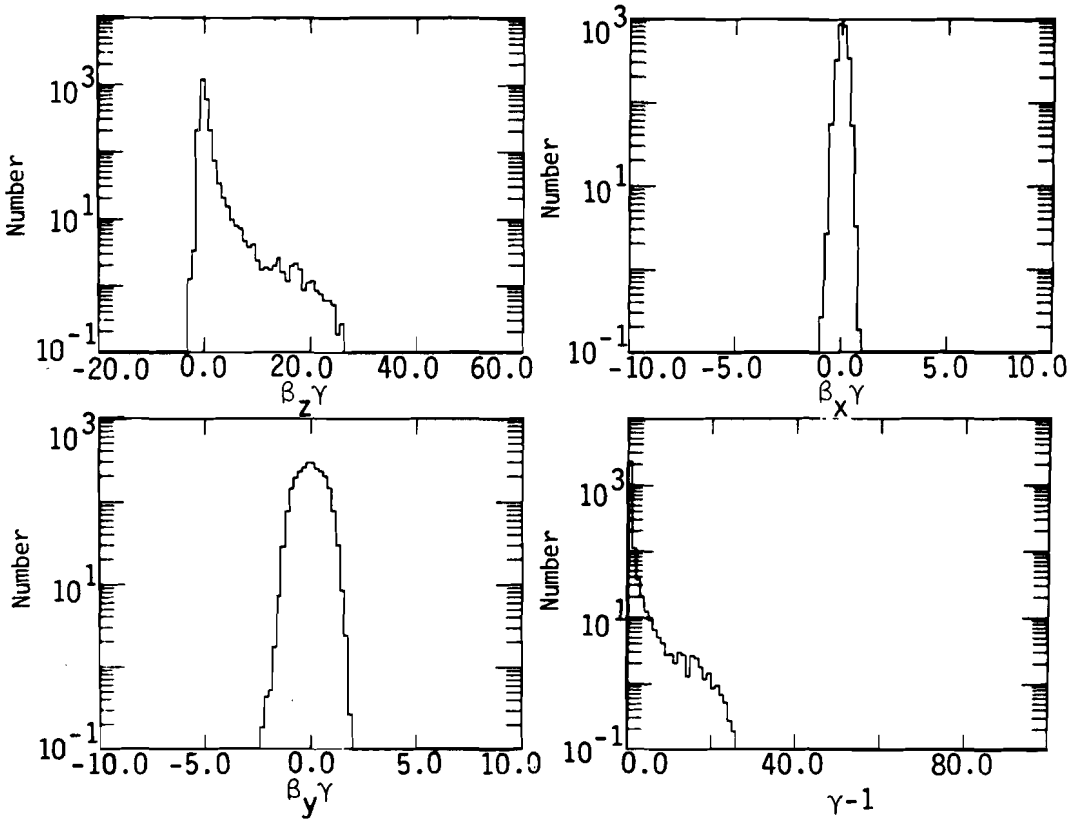

Figure 8. Plasma electron momentum distributions in x, y and z and energy distribution at $\tau = 120\ \omega_p^{-1}$. Parameters are $\omega_0 = 10.6\ \omega_p$, $\omega_1 = 9.5$, $E_0\ (0,1) = 5.0\ mc\omega_p/e$. Initially, $T_e = 10$ keV.

High intensity laser pulses ($v_{osc}/c > 1$) result in plasmas where relativistic effects may be of comparable importance. This results in the forward Raman scattered wave having a frequency, ω_s, not equal to ω_1. Likewise, the cascade process to lower frequencies due to multiple Raman Scattering results in $\omega_p \neq \Delta\omega \equiv \omega_o - \omega s$. Although RFS still takes place, the two laser pulses no longer reinforce each other. Note also that the γ_p associated with the plasma is a function of z. Thus, a range of scattering frequencies are present again leading to turbulence.

These combined processes lead to rapid loss of synchronism between the laser and plasma waves. Indeed, after a short time ($\tau = 120\ \omega_p^{-1}$) a plasma wave train is no longer discernible (see Figure 9). The deleterious effects, however, can be negated simply by lowering the laser intensity as little as a factor of two so that $E_o = mc\omega/e$ rather than $\sqrt{2}\ mc\omega/e$. A coherent train of plasma waves in both space and time can be generated under these conditions. This is apparent in Figures 10 and 5. By choosing the proper laser intensity the number of particles being accelerated can be adjusted to limit damping of the plasma waves. Thus, acceleration of a few particles to maximum energy can be maintained.

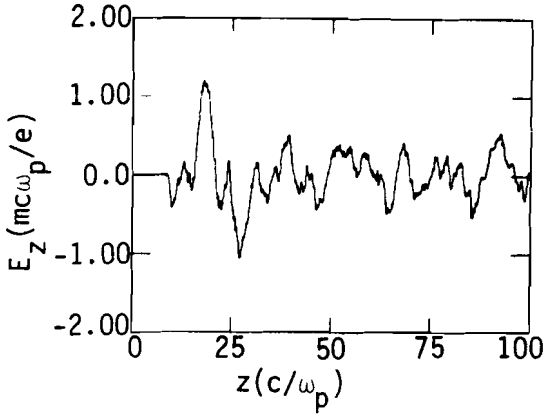

Figure 9. Longtudinal electric field as a function of distance, $\tau = 120\ \omega_p^{-1}$. Simulation parameters are $\omega_o = 5.0\ \omega_p$, $\omega_1 = 4.0\ \omega_p$, $E_o\ (0,1) = 2.8\ mc\omega_p/e$ and $T_e = 0$.

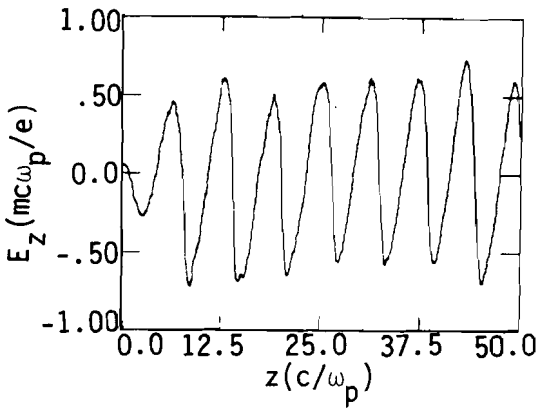

Figure 10. Longitudinal electric field as a function of distance, $\tau = 120\ \omega_p^{-1}$. Simulation parameters are $\omega_o = 10.6\ \omega_p$, $\omega_1 = 9.6\ \omega_p$, $E_o\ (0,1) = 5.0\ mc\omega_p/e$ and $T_e = 10$ keV.

FREQUENCY MATCHING

One of the practical problems facing the realization of a Plasma Beatwave Accelerator is the need to create a uniform plasma of a set density. However, the constraint may not be as stringent as it appears. In the RFS regime the frequency matching condition does not require $\omega_0 - \omega_1 = \omega_p$. Because of the cascade downward in frequency at intervals of ω_p due to multiple Raman Scattering and the cascade upward as a result of multiple four-wave interactions, frequency matching only requires $\omega_0 - \omega_1 = n\omega_p$.

In one code run, $\omega_0 = 10\ \omega_p$ and $\omega_1 = 8\ \omega_p$ was chosen so that $\Delta\omega = 2\omega_p$. After an initial period in which the plasma attempts to oscillate at $2\omega_p$, RFS of the ω_0 wave leads to an appreciable electromagnetic component at $\omega_2 = 9\ \omega_p$. Beating then occurs between ω_0 and ω_2, as well as, ω_1 and ω_2 to produce a large amplitude plasma wave. This is shown in Figure 11.

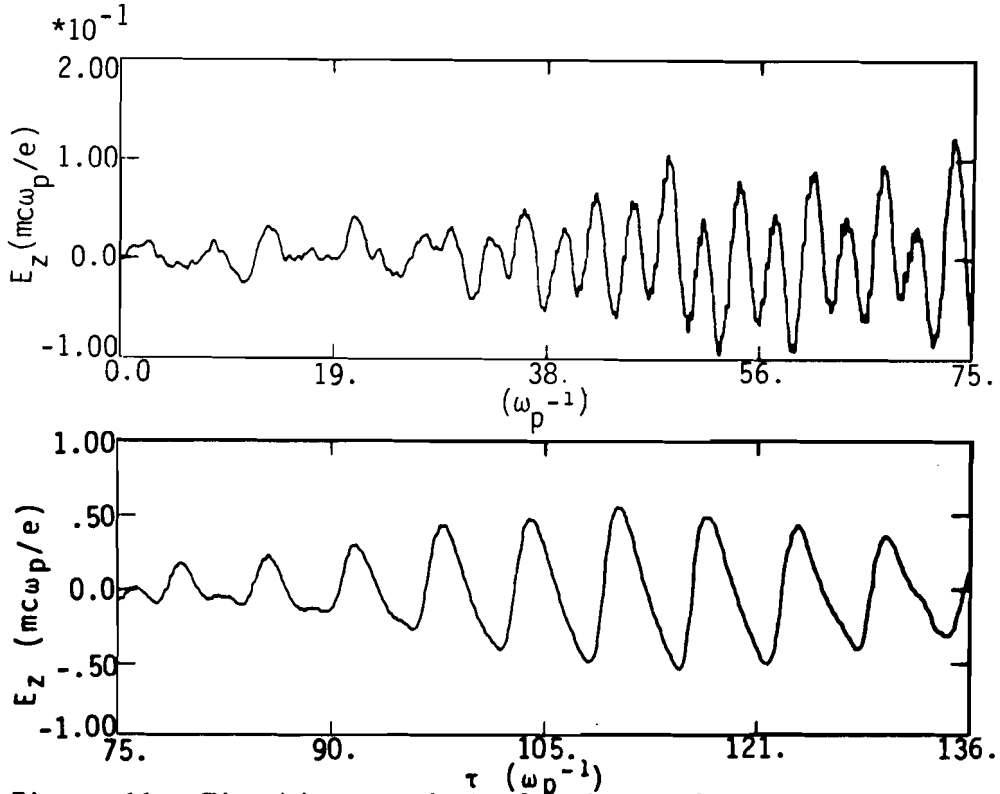

Figure 11. Time history of the longitudinal electric field inside the plasma from $\omega_p\tau$ = 0 - 136. Simulation parameters are ω_0 = 10.0 ω_p, ω_1 = 8.0 ω_p and E_0 (0,1) = 4.5 $mc\omega_p/e$.

Another consideration is determination of the plasma density fluctuation level which is tolerable. As noted earlier, optical mixing is sensitive to relatively low levels of temperature-induced noise. RFS at high intensities, however, produces large charge density bunches which are unaffected by fluctuation levels at a temperature of 10 keV. This may be explained in terms of the RFS intensity threshold for inhomogeneous plasmas derived in Reference 10. However, further correlation studies between instability growth and noise levels would be helpful.

STREAMING INSTABILITIES

One class of virulent instabilities which must be addressed for this accelerator are the various forms of streaming instabilities. As the particles are accelerated through the plasma, waves with a phase velocity equal to the beam velocity will grow. This only occurs, however, if the beam distribution superimposed on the plasma distribution is increasing ($\partial f/\partial v > 0$), where f is the distribution function. If the distribution is monotonically decreasing ($\partial f/\partial v < 0$) everywhere, then the plasma is absolutely stable against streaming instabilities.[12] This is the case where electrons are drawn out of the plasma to be trapped and energy distributions of the plasma electrons are monotonically decreasing and stable against the two-stream.

In the simulation modeling the CO_2 multi-band laser, ions with a mass ratio of $m_i/m_e = 359$ were included. The laser pulse has a risetime of 100 ω_p^{-1}. Admittedly, this is an artificially short risetime. However, it does allow a period, before electron trapping can take place, for the ions to react to the laser pulse and create unwanted density fluctuations and a nonthermal ion distribution. This does not occur. The ions do not react to the electromagnetic waves even at this fictitiously low mass ratio. The plasma distribution remains stable against ion-electron as well as electron-electron two-stream instabilities. The real concern with regard to streaming instabilities is related to preaccelerated particles injected into the plasma. The distribution will be susceptible to the relativistic two-stream instability. However, its effects may be mitigated by the presence of large amplitude plasma waves at approximately the same phase velocity. Also, the injected particles can be at densities orders of magnitude below the background plasma so that the instability growth rate will be low.

SIMULATION WITH PREACCELERATED PARTICLES

In an attempt to answer some of these questions, a 1 MeV electron beam with a density of 10^{14} cm^{-3} was coinjected with a 10^{16} W/cm CO_2 laser emitting at 10.6 μm and 9.6 μm. Thus, the beam to plasma density ratio was .001. The plasma was cold. As before, a small number of plasma electrons are trapped and accelerated resulting in a monotonically decreasing distribution. Because the electron beam was not bunched at injection, its accelerated emittance is large. Notably, the beam particles bunch at a phase in the wave which is different from the plasma electron bunches. Yet no streaming instability results. A more conclusive test using prebunched, monoenergetic ions at a laser intensity which does not allow plasma trapping will be conducted shortly. Plots of various quantities of interest are given in Figure 12. The total longitudinal distance is 2 mm for the given plasma density. Of interest is the peak charge density. It is a factor of as high as 3 above its initial value indicating the magnitude of the charged particle bunching taking place.

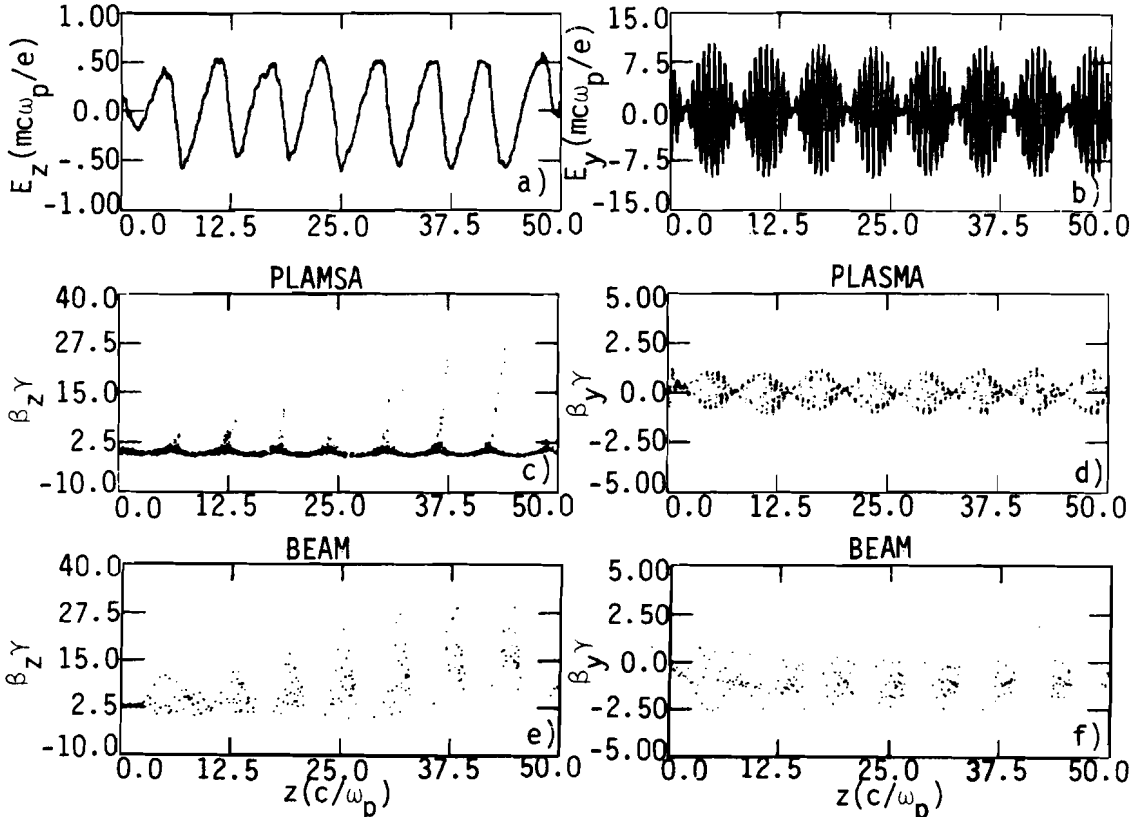

Figure 12. Plots of a) plasma wave electric field, b) laser electric field, c) plasma electron longitudinal, d) plasma electron transverse, e) beam longitudinal, and f) beam transverse momentum phase spaces at $\omega_p\tau$ = 74.0. Simulation parameters are ω_o = 10.6 ω_p, ω_1 = 9.6 ω_p, E_o (0,1) = 5.0 $mc\omega_p/e$ and T_e = 0 keV.

SUMMARY

This paper has attempted to convey a number of salient features of the Plasma Beatwave Accelerator utilizing results from one-dimensional, relativistic, electromagnetic simulations. The beatwave, which is constructed by parallel propagation of two laser pulses, is a practical means of creating large amplitude plasma waves. The accelerating plasma field is on the order of $mc\omega_p/e$. Nonlinear wave-wave processes are responsible for plasma wave growth. If $\omega_0 - \omega_1 = \omega_p$, optical mixing may be used to enhance the Raman Forward Scattering Instability and drastically reduce the intensity necessary to excite large electrostatic waves. Wave synchronism is maintained provided particle trapping does not damp the wave and produce a turbulent plasma. This implies a combined $v_{osc}/c \leq 1$. In this same intensity range some plasma particle trapping and acceleration appear to be beneficial in suppressing streaming instabilities. Freqency matching in the RFS regime only requires that $\omega_0 - \omega_1 = n\omega_p$. The downward and upward cascade at ω_p intervals produces the beatwave conditions necessary to create the plasma waves.

A number of practical considerations in applying this concept to high energy accelerators deserve mention,[14] aside from the very high field strengths. The acceleration takes place far from any material structures. The medium it is operating in cannot breakdown, since it is already fully ionized. The particle acceleration takes place in the same direction as the laser pulse is propagating. Finally, extremely high energy (TeV) laser particle accelerators require staging, because of the limited range over which the laser beam can maintain a focus. Here, the Plasma Beatwave Accelerator has a significant advantage. The acceleration takes place in a plasma wave rather than in vacuum. Therefore, if ω_0, $\omega_1 \gg \omega_p$, the problem of phase locking the accelerated particles from one accelerator to another is greatly reduced, because of the difference between the optical and plasma wavelengths. This concept is still in an embryonic stage. Theoretically, the main unanswered questions concern the transverse dynamics and self-fields of the beam. These must be addressed using fully two-dimensional and in some cases three-dimensional simulations. A partial list of these issues is given here.

Does the particle beam pinch or expand radially under the influence of its combined azimuthal-magnetic and radial electric fields? If the plasma return current flows inside the beam channel, the self-magnetic

field generated by the net current may be too weak to overcome the beam's radial electric field: The beam will expand radially. On the other hand, if the return current flows outside the beam channel and $n_i/n_e > 1/\gamma^2$ (almost certainly true), the beam will pinch due to its azimuthal magnetic self-field.

How does diffraction of the laser pulse in the focal region affect its intensity, plasma wave amplitude and particle acceleration? Laser self-channeling due to the radial ponderomotive force will decrease the plasma density in the beam channel and destroy the frequency matching condition. Can it be overcome if $\tau_{pulse} < r_{spot}/C_s$, where r_{spot} is the laser focal spot size radius and C_s is the ion acoustic velocity? Raman backscatter is suppressed by Landau damping in a hot plasma.[2-4,9] Will Raman sidescatter be similarly suppressed or will it increase beam emittance and/or grow faster than Raman Forward Scattering? Will the particle beam break up due to filamentation instabilities?

All of these questions are critical for a high energy physics accelerator, due to multiple plasma stages and low beam emittance necessary for conducting research.

ACKNOWLEDGEMENT

The authors would like to thank Drs. A. Sessler, M. Tigner, and W. Willis for many helpful discussions on current accelerator technology and issues. We are particularly indebted to Drs. C. Joshi and T. Tajima for useful talks on optical mixing, nonlinear wave damping and experimental techniques. This work was supported by the Air Force Weapons Laboratory under contract F29601-78-C-0082.

REFERENCES

1. T. Tajima and J. M. Dawson, Phys. Rev. Lett. 43, 267 (1979).
2. T. Tajima and J. M. Dawson, IEEE Trans. Nuc. Sci. NS-28, 3416 (1981).
3. C. Joshi, in Laser Acceleration of Particles, edited by P. J. Channell, (AIP Conference Proceedings, No. 91, New York, 1982), p. 28.
4. T. Tajima and J. M. Dawson, in Laser Acceleration of Particles, edited by P. J. Channell, (AIP Conference Proceedings, No. 91, New York, 1982), p. 69.
5. D. J. Sullivan and B. B. Godfrey, IEEE Trans. Nuc. Sci. NS-28, 3395 (1981).
6. D. J. Sullivan and B. B. Godfrey, in Laser Acceleration of Particles, edited by P. J. Channell, (AIP Conference Proceedings, No. 91, New York, 1982), p. 43.
7. B. I. Cohen, A. N. Kaufman, and K. M. Watson, Phys. Rev. Lett. 29, 581 (1972).
8. M. N. Rosenbluth and C. S. Liu, Phys. Rev. Lett. 29, 701 (1972).
9. C. Joshi, T. Tajima, J. M. Dawson, H. A. Baldis, and N. A. Ebrahim, Phys. Rev. Lett. 47, 1285 (1981).
10. K. Estabrook, W. L. Kruer, and B. F. Lasinski, Phys. Rev. Lett. 45, 1399 (1980).
11. D. Eimerl, R. S. Hargrove, and J. A. Pasiner, Phys. Rev. Lett. 46, 651 (1981).
12. C. S. Gardner, Phys. Fluids 6, 839 (1963).
13. J. M. Dawson and R. Shanny, Phys. Fluids 11, 1506 (1968).
14. These criteria were put forward by R. Pantell at the Laser Particle Accelerator Workshop (LANL, February 1982).

DISCUSSION

Winterberg. Professor Salam tells us that he needs about 100 TeV, that is, about 1000 ergs per particle. Now if we have not just a toy but an accelerator with good luminosity able to make sufficient number of reactions, I assume that we need about 10^{13} particles. This is 1000 MJ. If we liberally assume 10% efficiency for the accelerator this gives 10,000 MJ! No laser in sight can produce this (though electron beams might). Although the plasma physics is very interesting, I have my doubts that this will lead to an accelerator that meets the needs of high energy physics.

Sullivan. You have raised the general question of energy balance, and how one can produce high energy and high luminosity with a laser. I am not going to try to answer that now.